Olefination and group transfer reactions of an electron deficient tantalum methylidene complex†

Sarah M. Mullins, Robert G. Bergman* and John Arnold*

Received 9th September 2005, Accepted 19th October 2005
First published as an Advance Article on the web 14th November 2005
DOI: 10.1039/b512741f

The reactivity of an electronically unsaturated tantalum methylidene complex $[TolC(NSiMe_3)_2]_2$-$Ta(CH_2)CH_3$ (**1**) supported by $[TolC(NSiMe_3)_2]$ amidinate ligands is described. Electrophilic addition and olefination reactions of the $Ta{=}CH_2$ functionality are reported. Alkylidene **1** participates in group-transfer reactions not observed in sterically similar, but electronically saturated, analogues. Reactions with substrates containing unsaturated C–X (X = C, N, O) bonds yield [Ta]=X compounds and vinylated organic products; carbon–sulfur cleavage reactions to produce tantalum thioformaldehyde and tantalum sulfido complexes.

Introduction

Transition-metal methylidene complexes are important in both industrial and synthetic organic applications. For example, surface-bound methylene groups are proposed as intermediates in the Fischer–Tropsch reaction.[1,2] Heteroatom (O, S, NR) abstraction reactions by methylidene complexes model hydrodesulfurization and hydrodeamination of petroleum feedstocks as well as the poisoning of catalyst surfaces.[3] Molecular compounds that are analogous to the industrially important methylene-functionalized metal and metal oxide surface species provide insight into the structure and reaction mechanisms of these complicated heterogeneous systems.[4] Finally, transition-metal methylidene complexes are useful reagents for organic transformations.[5] Insertion of the carbene fragment into C–H bonds is one method for the functionalization of organic molecules.[6] As a result of these applications, the chemistry of transition-metal methylidene complexes is now well established.

While early metal methylidene complexes are unquestionably of great industrial and academic significance, their synthesis is often a challenge. In most early metal alkylidene complexes, the $M{=}CR_2$ moiety tends to be quite unstable to decomposition and dimerization. Accordingly, the isolation of such compounds often requires steric bulk at the metal, a high formal electron count, or substitution at the α-carbon atom. These strategies have been employed by Schrock and co-workers,[7] who used electronic saturation to synthesize $Cp_2Ta(CH_2)CH_3$[8,9] and a bulky substituent on the alkylidene carbon atom to prepare $CpCl_2Ta(CHCMe_3)$.[10] While the 18-electron $Cp_2Ta(CH_2)CH_3$ reacts with some organic electrophiles,[8] the less electron rich tantalum alkylidenes (*e.g.* $14e^-$ $CpCl_2Ta(CHCMe_3)$) exhibit the most reactivity.[7,11] Electronically unsaturated titanium methylidenes, which also exhibit a broad spectrum of reactivity with organic substrates, may be accessed from "masked" precursors, such as the aluminium alkyl-stabilized Tebbe reagent[12] or titanacyclobutanes.[13] Despite the potential increased reactivity of these derivatives compared to that of the saturated complexes, the chemistry of isolable electronically unsaturated transition-metal methylidene complexes remains largely unexplored.[14–19]

The α-carbon atoms of transition-metal methylidene complexes have been reported to exhibit either nucleophilic or electrophilic behavior. The electronic properties of these unsaturated ligands are highly sensitive to electronegativity of the metal, its oxidation state, and the overall charge of the complex.[5] Generally, high oxidation state early metal carbenes exhibit nucleophilic behavior, while low oxidation state late metal carbenes generally act as electrophiles.[20] However, these observations are far from rigid, and methylidenes are especially sensitive to the electron density at the metal center. For example, the late metal methylidene, $Cp^*(PMe_3)Ir(CH_2)$, exhibits nucleophilic behavior.[21] The nucleophilic methylidene in $Cp_2Ta(CH_2)CH_3$ stands in contrast to the electrophilic nature of the isoelectronic, cationic tungsten analogue, $[Cp_2W(CH_2)CH_3]^+$.[22] Some methylidene complexes even exhibit amphiphilic behavior: an example is $Cl(NO)PPh_3Os{=}CH_2$, which reacts with both electrophiles (H^+) and nucleophiles (CO or CNR).[23]

Given the potential applications of electronically unsaturated transition-metal methylidenes, we were interested in exploring the reactivity afforded by the bis(amidinate)tantalum methylidene complex, $[TolC(NSiMe_3)_2]_2Ta(CH_2)CH_3$ (**1**), the synthesis of which we have previously reported.[24] The bis(trimethylsilyl)tolylamidinate ligand set enforces a *cis* geometry of the methylene and methyl ligands, which is important for potential migration processes, and provides steric bulk intermediate to that of bis(Cp) and bis(Cp*) ligand sets.[25] The anionic bis(trimethylsilyl)tolylamidinate ligand is generally considered to be a four electron donor; this generates an electronically unsaturated ($14e^-$) metal center in **1**.

Our previous mechanistic work on the reaction of tantalum methylidene **1** with pyridine *N*-oxides demonstrates that the electron deficient metal center is critical to opening new reaction pathways (Scheme 1).[26] The selective reactivity of **1** with pyridine *N*-oxides stands in contrast to the $18e^-$ tantalocene analog, $Cp_2Ta(CH_2)CH_3$, which is unreactive. Additional support for our belief that the electron count is important in this reaction comes from a recent report in which the $16e^-$ "$Cp_2Ti(CH_2)$" was used

Department of Chemistry, University of California, Berkeley, CA, USA 94720-1460

† In memory of our friend and colleague Professor Ian Rothwell.

Table 1 Crystallographic data and refinement details for **1**, **13**, **14** and **15**

	1	**13**	**14**	**15**
Empirical formula	$C_{30}H_{55}N_4Si_4Ta$	$C_{39}H_{64}N_5Si_4Ta$	$C_{30}H_{55}N_4Si_4STa$	$C_{29}H_{53}N_4Si_4TaS$
M_r	765.08	896.26	829.20	783.11
T/°C	−118	−103	−105	−107
Crystal system	Monoclinic	Monoclinic	Monoclinic	Monoclinic
Space group	$C2/c$ (no. 15)	$P2_1/c$ (no. 14)	$C2/c$ (no. 15)	$C2/c$ (no. 15)
a/Å	28.2182(1)	17.9014(4)	12.9195(3)	28.2627(4)
b/Å	8.7227(1)	11.6015(2)	18.8911(4)	8.7781(2)
c/Å	19.8359(1)	23.0038(5)	16.7243(2)	19.8801(3)
V/Å^3	3814.35(6)	4459.0(2)	3970.3(1)	3819.2(1)
β/°	128.625(1)	111.041(1)	103.423(1)	129.253(1)
Z	4	4	4	4
D_c/g cm^{-3}	1.332	1.335	1.387	1.362
Scan type/°	ω, 0.3	ω, 0.3	ω, 0.3	ω, 0.3
Frame collection time/s		10		10
2θ range/°	3–52.3	3–52.0	3–51.9	3–49.4
μ/mm^{-1}	30.26	26.00	30.14	30.77
T_{max}, T_{min}	0.640, 0.450	0.636, 0.517	0.817, 0.580	0.496, 0.223
Crystal dimensions/mm	0.20 × 0.20 × 0.30	0.12 × 0.25 × 0.30	0.10 × 0.12 × 0.12	0.20 × 0.15 × 0.25
No. reflections measured	10633	21557	9490	8561
No. unique reflections	3656	8314	3582	3355
No. observations ($I > 3\sigma$)	2920	4578	2562	2646
No. variables	177	442	173	181
Data/parameter	16.5	10.4	14.8	14.6
R_{int} (%)	2.7	4.6	6.2	4.6
R (%)	3.0	2.7	4.2	3.4
R_w (%)	3.7	3.0	5.2	3.9
GOF	1.42	0.93	1.47	1.4
Largest diff. peak, hole/e Å^{-3}	1.59, −0.94	0.76, −0.73	1.52, −1.13	0.72, −2.39

Reflections measured: hemisphere; refinement method: full-matrix least-squares on F^2; hydrogen atoms: idealized positions.

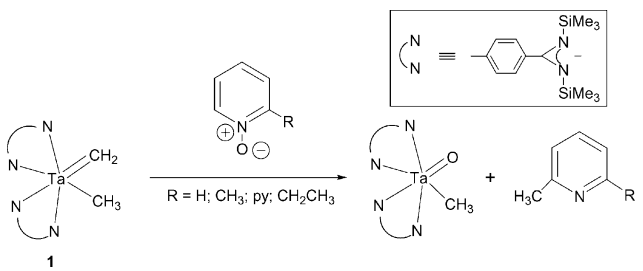

Scheme 1

to carry out an analogous pyridine *N*-oxide to methylpyridine transformation. This report also described the application of this methodology to a natural product synthesis.[27,28]

These reactions encouraged us to determine whether the thermodynamic stability of early metal–heteroatom (O, NR, S) multiple bonds can be coupled with carbene transfer to selectively functionalize organic substrates. This report describes how the tantalum methylidene **1** participates not only in familiar electrophilic addition and olefination reactions, but also group transfer reactions not observed in sterically similar, but electronically saturated, analogues.

Results and discussion

Solid-state structure of 1

The X-ray structure of **1** provides a starting point for analysis of the steric characteristics of the bis(trimethylsilyl)tolylamidinate ligands. An ORTEP diagram of **1** is shown in Fig. 1. Selected crystal and refinement data are in Table 1; bond lengths and angles for

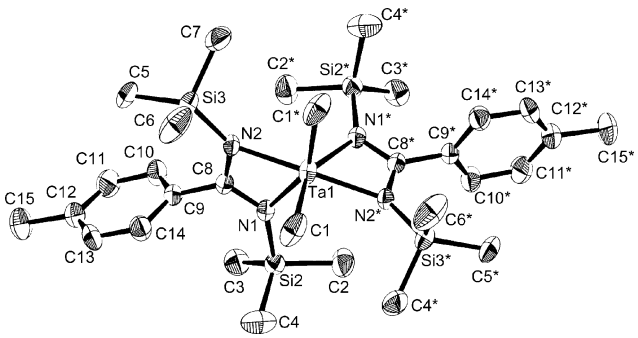

Fig. 1 ORTEP diagram of **1**, showing 50% probability ellipsoids. Hydrogen atoms are omitted for clarity.

1 are given in Table 2. The dominance of the bis(trimethylsilyl)-tolylamidinate ligands in the tantalum coordination sphere is not only evident visually, but is also reflected by the inability to crystallographically distinguish between the CH_2 and CH_3 ligands. Molecules of **1** have packed in a mixture of two enantiomers, resulting in a crystallographic C_2 axis which bisects the $(CH_3)Ta(CH_2)$ vector (despite the lack of molecular C_2 symmetry). The observed

Table 2 Selected bond distances (Å) and angles (°) for **1**

Ta(1)–N(1)	2.260(3)	N(1)–Ta(1)–N(2)	60.4(1)
Ta(1)–N(2)	2.191(3)	N(1)–Ta(1)–C(1)	92.7(2)
Ta(1)–N(5)	1.996(4)	N(2)–Ta(1)–C(1)	102.6(2)
Ta(1)–C(1)	2.049(5)	N(1)–C(8)–N(2)	114.7(3)
N(1)–C(8)	1.313(5)		
N(2)–C(8)	1.347(5)		

Ta1–C1 bond length, 2.05 Å, is an average of the normal metal–carbon single and double bond lengths.[5]

A space-filling model of **1** shows that the bis(trimethylsilyl)-tolylamidinate ligand set has a roughly rectangular shape and that the majority of the ligands' steric bulk is relatively distant from the methyl and methylidene groups (Fig. 2). Using CPK models, Teuben and co-workers determined the coordination aperture[29] to be 84° for $[PhC(NSiMe_3)_2]_2M$, compared to 103 and 72° for the metallocene analogues Cp_2M and Cp^*_2M (M = Y).[25] This result indicates that the steric bulk of the bis(tolylamidinate) ligand set is more similar to the bis(Cp*) set. A qualitative comparison of **1** and $Cp_2Ta(CH_2)CH_3$ (Fig. 2) reveals that the open faces of the complexes are more similar than might be expected for two ancillary ligand sets of such different size and shape.

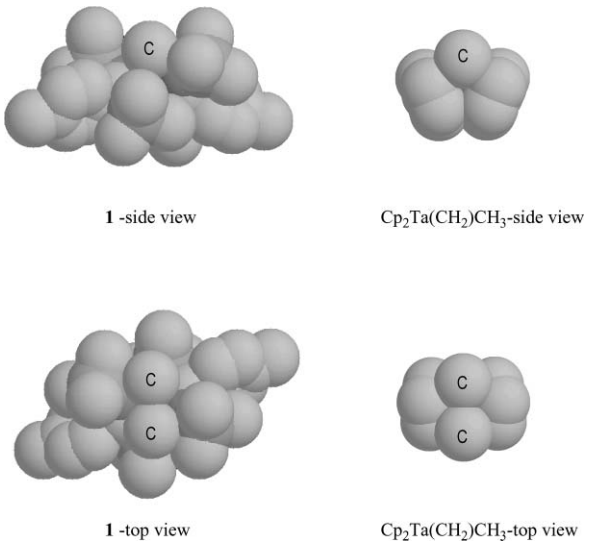

1 -side view $Cp_2Ta(CH_2)CH_3$-side view

1 -top view $Cp_2Ta(CH_2)CH_3$-top view

Fig. 2 Side and top views of space filling models for **1** and $Cp_2Ta(CH_2)CH_3$. Carbon labels identify the CH_2 and CH_3 ligands.

Reactions of 1 with electrophiles

The nucleophilic nature of the methylidene moiety of **1** is evident from its reactions with electrophilic alkylating reagents. The addition of 1 equiv. of methyl iodide to **1** results in the formation of the ethyl methyl iodo tantalum complex **2**, presumably by initial attack of the Me^+ fragment at the carbene carbon atom (Scheme 2). No reaction was observed between **1** and *tert*-butyl chloride or trimethylsilyl chloride.

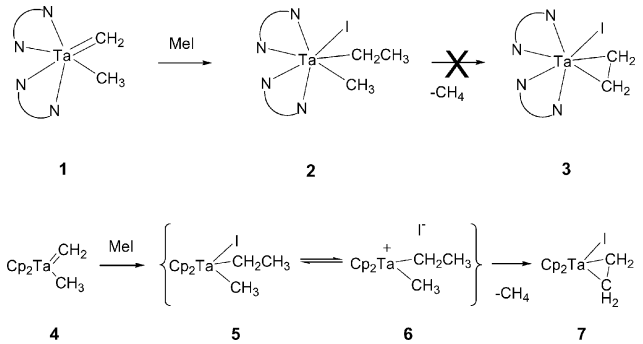

1 **2** **3**

4 **5** **6** **7**

Scheme 2

Differences in the reactions of methyl iodide between the analogous 14e⁻ (**1**) and the 18e⁻ ($Cp_2Ta(CH_2)CH_3$) complexes provide evidence for the relatively electrophilic nature of the tolylamidinate-supported tantalum complex (Scheme 2). In the tantalocene example, iodide may dissociate from the ethyl methyl iodido intermediate (**5**–**6**). β-Hydride elimination followed by reductive elimination of methane forms the ethylene iodide tantalocene complex (**7**).[8] No such dissociation or elimination reactions were observed for **2**; no methane or ethylene was observed, even upon decomposition of **2**. Presumably, the highly electrophilic tantalum favors more rapid attack of I^- after the initial alkylation, and subsequently disfavors the iodide dissociation required for the conversion of **2** to **3**.

Olefination reactions

Perhaps the most well-known reactions of early metal carbenes are those that yield organic molecules that contain unsaturated C–C bonds.[30] Not surprisingly, the methylidene complex **1** also participates in a variety of these reactions. For example, **1** reacts with nitriles (**8a**,**b**) to form vinylimido tantalum complexes (**11a**,**b**) (Scheme 3). The vinyl group is clearly evident in the ^1H NMR (δ 5.27 (d), 5.34 (d) ppm) and DEPT-135 (δ 105.3 ppm) experiments.

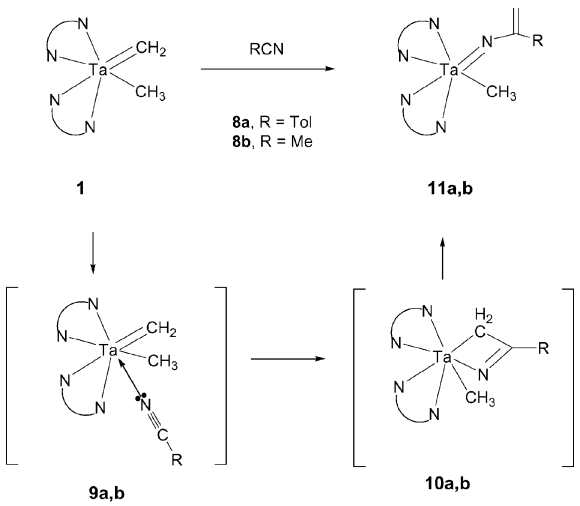

1 **11a,b**

9a,b **10a,b**

Scheme 3

The reaction is proposed to proceed first with nitrile coordination (**9a**,**b**), followed by formation of an azatantalacyclobutene (**10a**,**b**). Cycloreversion to the thermodynamically stable Ta=NR compound yields the product (**11a**,**b**) (Scheme 3). No intermediates were observed when the reaction was monitored by ^1H NMR spectroscopy; however, similar mechanisms have been suggested for the reactions of other tantalum alkylidenes with nitriles. Schrock and co-workers found that the 14e⁻ $CpCl_2Ta(CH^tBu)$[10] and 10e⁻ $(^tBuCH_2)_3Ta(CH^tBu)$[31] undergo this reaction with nitriles, whereas electronically saturated $Cp_2Ta(CH_2)CH_3$[8] and $Cp_2Ta(CH^tBu)Cl$[32] do not react at all. This suggests that nitrile coordination may be the first step in all of these reactions.

Complex **1** reacts with certain aldehydes to yield olefinated organic products. For example, the addition of acetaldehyde to a benzene-d_6 solution of **1** yields the tantalum oxo complex **12**[26] and propylene. However, no reaction is observed between

1 and carbonyl-containing substrates with larger substituents, such as tolualdehyde or benzophenone (Scheme 4). These [2 + 2] cycloaddition/reversion transformations are well-established for tantalum carbenes and phosphorus ylide complexes.[33–35]

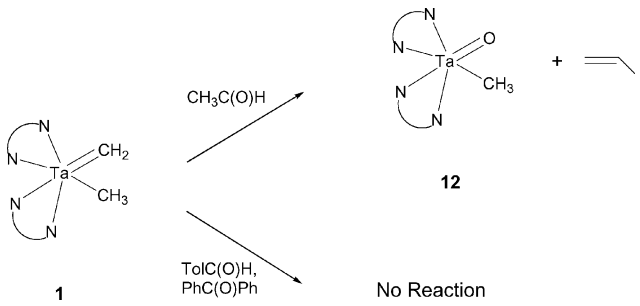

Scheme 4

When a benzene-d_6 solution of **1** was exposed to small alkenes (ethylene or propylene, 1 equiv. to 1 atm), complex mixtures of organic and organometallic products were obtained. Propylene and 1-butene were among the organic products identified by ^{1}H NMR and GC-MS. Attempts to isolate the tantalum-containing product(s) were unsuccessful, even when the reaction was carried out in the presence of added Lewis base. Carbene fragment insertion into small alkenes was previously observed in pincer[27] and cyclopentadienyl tantalum neopentylidene complexes.[36]

Reaction with isocyanide: Formation of a metal-bound ketenimine

Metal-ketenimine complexes are versatile building blocks for the synthesis of heterocyclic complexes. While carbene addition to an isocyanide is an established method for the synthesis of metal–ketenimine complexes, examples of this reaction with early metal carbenes have not been forthcoming.[37] Consequently, we tested the behavior of **1** with isocyanides.

The reaction of **1** with *tert*-butyl isocyanide yields multiple intractable products. In contrast, addition of 1 equiv. of 2,6-dimethylphenyl isocyanide to **1** yields the η^2-ketenimine complex **13** (eqn (1)). The ^{1}H NMR spectrum of complex **13** reveals two singlets, at δ 4.78 ppm (1H) and δ 5.99 ppm (1H). A ^{13}C–^{1}H HMQC experiment revealed that both protons correlate to a single resonance in the ^{13}C NMR spectrum (δ 77.2 ppm) (Fig. 3). A DEPT-135 experiment confirmed that this carbon resonance is the CH_2 group of the ketenimine. We presume that the two-bond coupling of these protons is too small to be observed.

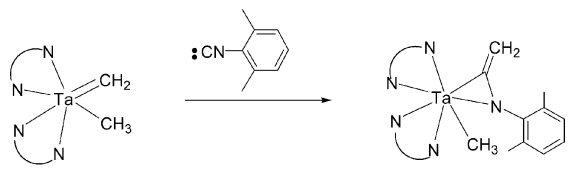

(1)

The X-ray structure of **13** establishes the regiochemistry of the ketenimine in the solid state and helps to explain the ^{1}H NMR spectrum. An ORTEP diagram of **13** is presented in Fig. 4. Metrical information is in Table 3; selected crystal and refinement data are in Table 1. The complex has a distorted capped trigonal prismatic geometry (Fig. 5). C39 is the capping ligand; three of the amidinate nitrogen atoms (N1, N2, N4) and the ketenimine nitrogen (N5) form the rectangular face. The tantalum atom sits 0.09 Å below the plane defined by these four nitrogen atoms (average nitrogen deviation from least squares plane = 0.03 Å). The remaining amidinate nitrogen atom, N3, and the ketenimine carbon, C29, form the third vertices of the triangular faces. The C29–N5 bond distance (1.380(7) Å) is consistent with the presence of a single bond (lit. C(sp^2)–N(sp^2) = 1.355 Å).[38] The very different

Table 3 Selected bond distances (Å) and angles (°) for **13**

Ta(1)–N(1)	2.123(4)	N(1)–Ta(1)–N(2)	61.1(2)
Ta(1)–N(3)	2.164(4)	N(2)–Ta(1)–N(4)	91.0(2)
Ta(1)–N(5)	1.996(4)	N(3)–Ta(1)–N(4)	60.6(2)
Ta(1)–C(39)	2.188(6)	N(4)–Ta(1)–N(5)	87.9(2)
N(5)–C(29)	1.379(7)	N(1)–Ta(1)–N(5)	119.6(2)
C(29)–C(30)	1.364(7)	N(3)–Ta(1)–C(29)	92.3(2)
Ta(1)–N(2)	2.296(4)	N(5)–C(29)–C(30)	130.4(5)
Ta(1)–N(4)	2.284(4)	Ta(1)–C(29)–N(5)	66.1(3)
Ta(1)–C(29)	2.106(5)	Ta(1)–N(5)–C(29)	74.7(3)
N(1)–C(1)	1.347(6)	N(1)–C(1)–N(2)	114.5(4)
N(2)–C(1)	1.329(6)	N(3)–C(15)–N(4)	114.0(5)
N(3)–C(15)	1.359(6)		

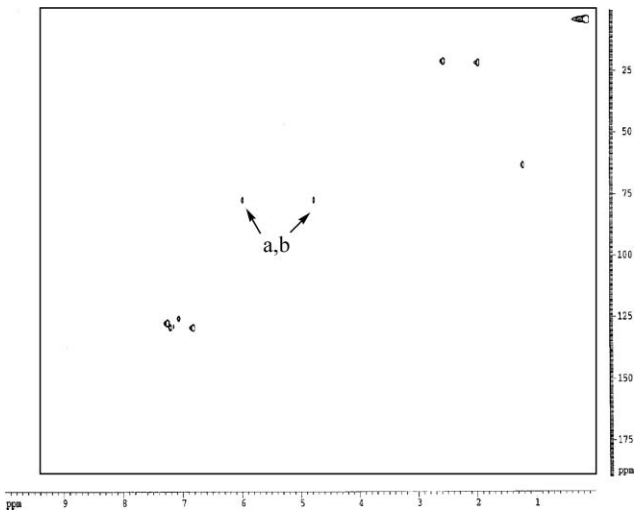

Fig. 3 ^{1}H–^{13}C HMQC spectrum of **13** at room temperature.

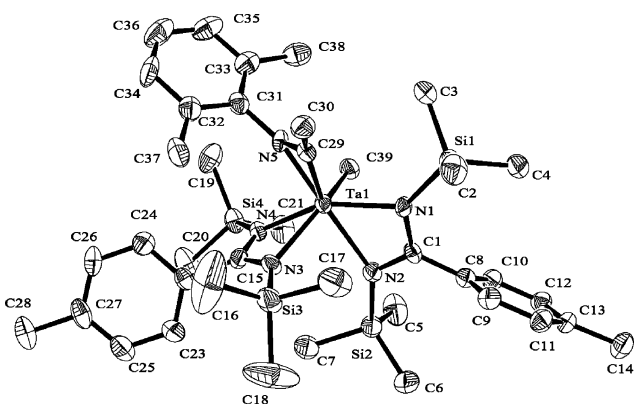

Fig. 4 ORTEP diagram of **13**, showing 50% probability ellipsoids. Hydrogen atoms are omitted for clarity.

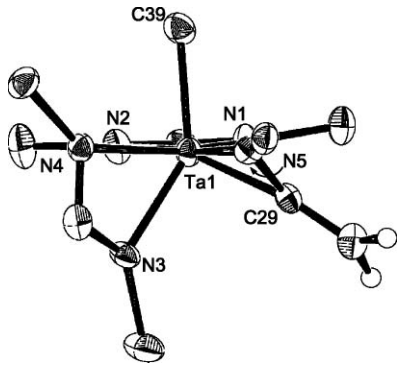

Fig. 5 ORTEP diagram of the immediate coordination sphere of **13**. Trimethylsilyl and aryl groups omitted for clarity.

chemical environments for the two methylene protons of the ketenimine moiety are apparent from this structure. Proton a is clearly oriented toward the trimethylsilyl group of the amidinate, whereas proton **b** points toward the aryl group of the ketenimine (Fig. 5).

Variable-temperature ^{1}H NMR spectra of **13** reveal that while multiple intramolecular fluxional processes occur, the methylene group orientation is preserved in solution. At room temperature, fast exchange of the bis(trimethylsilyl)tolylamidinate ligands is evident from the presence of a single trimethylsilyl resonance and a single tolyl methyl group resonance. At −70 °C, two tolyl methyl group resonances (c, d; see Fig. 6) are observed, suggesting slow exchange between amidinate ligands. Three trimethylsilyl resonances (e, f, g) are observed in a 18H : 9H : 9H integration ratio. This implies that rotation about the internal C_2 axis[39] of one amidinate ligand is slow, while for the second amidinate the rotation barrier is more rapid. The line drawing of **13**, based on the X-ray structure (Fig. 6), shows the two different chemical environments of the amidinate ligands. The large 2,6-dimethylphenyl substituent on the ketenimine hinders the rotation of the amidinate containing N3 and N4, whereas the N1, N2 amidinate is unencumbered and can rotate freely.[40] Hindered rotation of the 2,6-dimethylphenyl group is also observed at low temperature, leading to two methyl resonances (h, i), and is consistent with the slow exchange-limit structure. A ^{1}H NMR spectrum at the slow exchange limit is shown in Fig. 6.

Sulfur transfer reactions

As part of an exploration of carbon-sulfur bond cleavage reactions, we investigated the reactivity of **1** towards several sulfur-containing organic compounds. Tantalum methylidene **1** abstracts sulfur from propylene sulfide to yield the η^2-thioformaldehyde compound **14** and propylene (eqn (2)). The methylene protons of **14** appear as a singlet resonance at δ 2.87 ppm (2H), in the ^{1}H NMR spectrum. A resonance at δ 71.1 ppm in the ^{13}C{^{1}H} NMR spectrum was identified as the methylene carbon of the thioformaldehyde ligand by a DEPT-135 experiment.

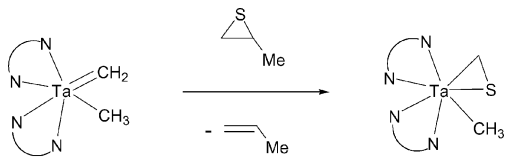

1 **14** (2)

Complex **14** crystallizes in the centrosymmetric space group $C2/c$. The η^2-thioformaldehyde ligand is bound as a metallathiacyclopropane, with the sulfur in the inside position. An ORTEP diagram is shown in Fig. 7. Selected crystal and refinement data are in Table 1; metrical parameters are given in Table 4. As in the X-ray structure of **1**, the superposition of enantiomers produces a crystallographic-C_2 axis, which leads to disorder in refinement of the $-CH_2S$ and $-CH_3$ groups. The sulfur atom of the thioformaldehyde (S1), which was disordered over two positions, was refined at half-occupancy. The carbon atoms of the methylene and the methyl group were refined as one full occupancy carbon (C12); see X-ray details for further information.

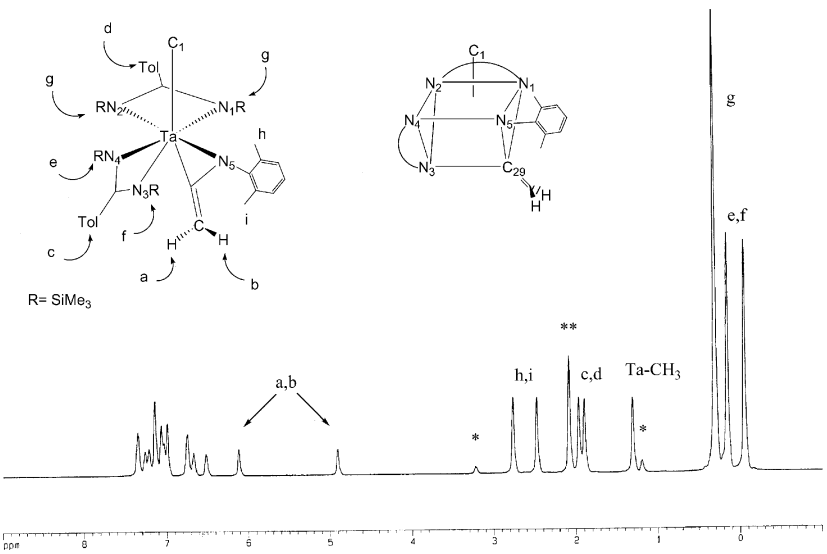

Fig. 6 ^{1}H NMR spectrum of **13** (toluene-d_8) at 203 K (* = residual diethyl ether, ** = solvent).

Table 4 Selected bond lengths (Å) and angles (°) for **14**

Ta(1)–S(1)	2.295(5)	S(1)–Ta(1)–N(1)	129.5(2)
Ta(1)–N(1)	2.281(6)	S(1)–Ta(1)–N(2)	104.8(2)
Ta(1)–N(2)	2.156(6)	S(1)–Ta(1)–C(15)	77.0(3)
Ta(1)–C(15)	2.23(1)	N(1)–Ta(1)–N(2)	61.0(2)
S(1)–C(15)	1.93(1)	N(1)–Ta(1)–C(15)	148.0(3)
N(1)–C(1)	1.31(1)	N(2)Ta(1)–C(15)	98.4(3)
N(2)–C(1)	1.355(9)	Ta(1)–S(1)–C(15)	63.0(3)
		Ta(1)–C(15)–S(1)	66.6(4)

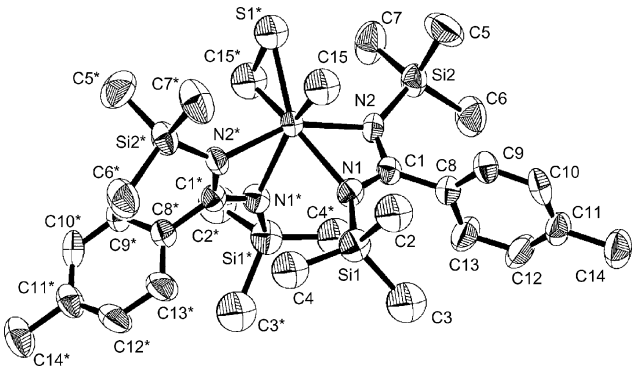

Fig. 7 ORTEP diagram of **14**, showing 50% thermal probability ellipsoids. Hydrogen, S1, C16/C16*, C17/C17*, and C18/C18* atoms (disordered sulfur atom and trimethylsilyl group) are omitted for clarity.

Compound **14** is one of only a few η^2-thioformaldehyde complexes known for early metals (Ta,[41] Zr[42] and Ti[43]). In addition, **14** is thermally robust; no changes were observed upon prolonged heating at 135 °C. This behavior contrasts to that of other tantalum thioaldehydes, $Cp_2Ta(SCHR)H$, which undergo facile migrations to the more thermodynamically stable terminal sulfido alkyl complexes, $Cp_2Ta(S)CH_2R$.[44]

Carbon–sulfur bond cleavage of a different kind occurs in the reaction of **1** with triphenylmethanethiol, to form the terminal sulfido complex **15** and triphenylethane (eqn (3)). The ^1H and $^{13}C\{^1H\}$ NMR spectra of the tantalum product are similar to those for the terminal tantalum oxo analog, **12**. The electron impact mass spectrum shows the molecular ion at m/z 782.

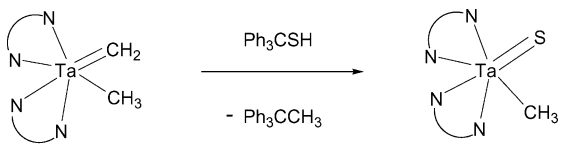

(3)

The structure of the terminal tantalum–sulfido complex was confirmed by X-ray crystallography. An ORTEP diagram is shown in Fig. 8. Selected crystal and refinement data are given in Table 1; metrical parameters are in Table 5. Like **1** and **14**, the sulfido complex **15** crystallizes in the centrosymmetric space group, $C2/c$. Again, the superposition of the two enantiomers produces a crystallographic C_2 axis. The sulfido and methyl groups are disordered over two positions; S1 and C15 were each refined at half-occupancy. The Ta1–S1 bond length is 2.22 Å, similar to other reported terminal Ta–S multiple bonds.[45,46]

Table 5 Selected bond lengths (Å) and angles (°) for **15**

Ta(1)–S(1)	2.222(10)	S(1)–Ta(1)–N(1)	153.7(2)
Ta(1)–N(1)	2.251(4)	S(1)–Ta(1)–N(2)	92.8(2)
Ta(1)–N(2)	2.144(3)	S(1)–Ta(1)–C(15)	95.4(7)
Ta(1)–C(15)	2.27(4)	N(1)–Ta(1)–N(2)	61.1(1)
N(1)–C(1)	1.320(5)	N(1)–C(1)–N(2)	114.6(4)
N(2)–C(1)	1.337(6)		

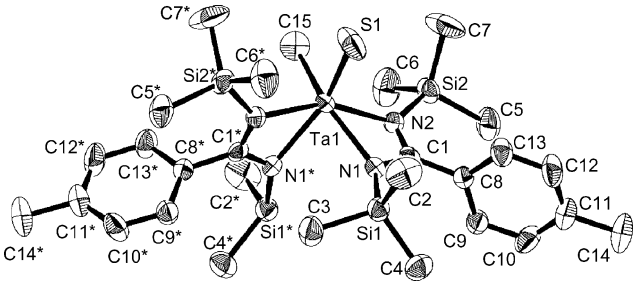

Fig. 8 ORTEP diagram of **15**, showing 50% thermal probability ellipsoids. Hydrogen atoms, C15* and S1* are omitted for clarity.

Several possible mechanisms for the formation of **15** and triphenylethane are outlined in Scheme 5. In mechanism A, the methylidene deprotonates the thiol to form the symmetrical intermediate **16**. β-Elimination reaction yields **15** and triphenylethane. In mechanism B, Ph_3CSH reacts as an electrophile (Ph_3C^+), attacking the nucleophilic methylidene to form intermediate **17**. β-Hydride transfer from the thiolate group yields **15** and triphenylethane. For pathway C, Ph_3C^+ abstracts the methide group to yield

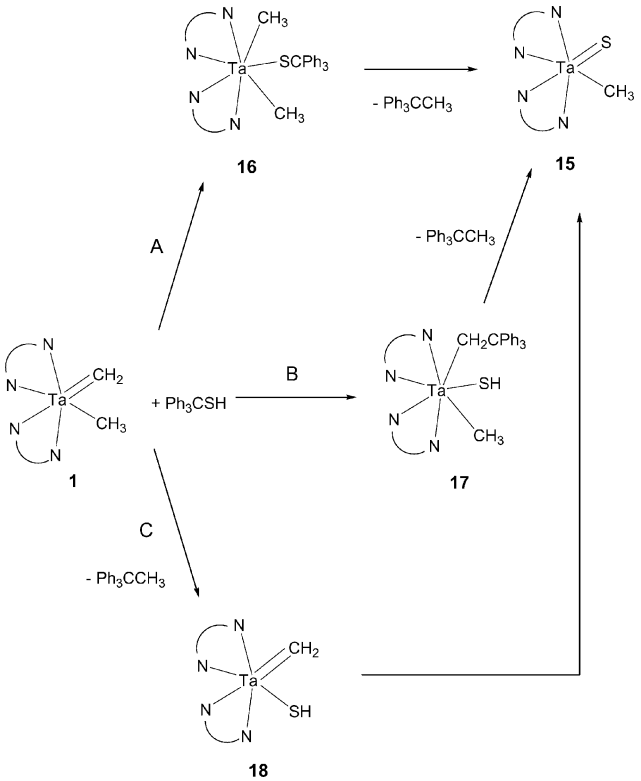

Scheme 5

triphenylethane and a tantalum methylidene thiolate intermediate (**18**). In the final step, **18** rearranges to the thermodynamically preferred tautomer (**15**).

While no intermediates were observed in this reaction, the three proposed mechanisms proceed through distinct intermediates that are distinguishable by performing a deuterium tracer experiment. The addition of 1 equiv. of triphenylmethanethiol (73%-d_1) to **1** yields a mixture of deuterium-incorporated products $[TolC(SiMe_3)_2]_2Ta(S)CH_2D$ (0.442 H), Ph_3CCH_3 (1.09 H), $[TolC(SiMe_3)_2]_2Ta(S)CH_3$ (1.15 H) and Ph_3CCH_2D (0.438 H).[47] When the relative integration values of these products are corrected to account for the incompletely deuterated starting material, a nearly statistical ratio of products is revealed ($TaCH_3$: $TaCH_2D = 1.07 : 1.00$, $Ph_3CCH_3 : Ph_3CCH_2D = 1.02 : 1.00$). These data are consistent with the intermediacy of **16** in mechanism A, which is also the only pathway expected to give a mixture of deuterated products. Furthermore, the observed isotopic distribution (*i.e.* lack of d_2 or d_3 products) suggests that the protonation reaction which forms **16** is irreversible.

Elimination reactions from tantalum(V) thiolate complexes have been reported. When β-hydrogens are present on the thiolate ligand, β-hydride elimination to thioformaldehyde is favored.[41] In the case of a tertiary substituted thiolate group, carbon-sulfur cleavage is preferred.[48,49] The latter is consistent with the proposed mechanism for the reaction between **1** and Ph_3CSH.

Oxygen abstraction reactions

Carbene complex **1** does not react with the oxygen analogs of the sulfur reagents discussed above (propylene oxide, Ph_3COH). We previously reported on the reactions of **1** with pyridine *N*-oxides and nitrones.[26]

Summary and conclusion

The bis(amidinate) ancillary ligands on the tantalum methyl methylidene complex **1** produce an electronically unsaturated ($14e^-$) tantalum center that has open space similar to that of early metal bent metallocenes. Tantalum methylidene **1** is a stable, isolable complex, but is reactive toward a range of electrophilic substrates. Reactions with substrates containing unsaturated C–X (X = C, N, O) bonds yield [Ta]=X compounds and vinylated organic products. Methylidene **1** participates in carbon-sulfur cleavage reactions to produce tantalum thioformaldehyde and tantalum sulfido complexes. The electrophilic character of the $14e^-$ tantalum center is important in this chemistry. The range of reactions reported herein for **1** expands the scope of transformations known for early metal methylidene complexes.

Experimental

General considerations

Standard Schlenk line and glove box techniques were used throughout. Hexanes was distilled from purple Na/benzophenone under nitrogen. Toluene and hexamethyldisiloxane (HMDSO) were distilled from Na under nitrogen. Benzene and pentane were dried by passage through activated alumina and then degassed with a nitrogen purge.[50] C_6D_6 was vacuum transferred from Na/benzophenone. Propylene sulfide (Aldrich) was first dried over molecular sieves, transferred under static vacuum to a Teflon-sealed flask and stored at 5 °C. Pyridine *N*-oxide and 2-methylpyridine *N*-oxide (Aldrich) were dried over molecular sieves in toluene and the crude solid sublimed before use. 2-Ethylpyridine *N*-oxide was synthesized starting from ethylpyridine *via* the literature procedure.[51] 2,2′-Dipyridyl *N*-oxide[52] was prepared according to literature procedures. Methyl iodide was stored over Cu wire. 1,3,5-Trimethoxybenzene (Aldrich) was sublimed before use. Ph_3CSH (Aldrich), 2,6-dimethylphenyl isocyanide (Fluka), and CH_3OTf (Aldrich) were used as received. Acetonitrile and *p*-tolylnitrile were distilled from CaH_2. Melting points were determined in sealed capillaries and are uncorrected. ^1H and $^{13}C\{^1H\}$ NMR spectra were recorded at ambient temperatures, unless otherwise noted. IR samples were prepared as mineral oil mulls and taken between KBr plates. Elemental analysis and mass spectral data were determined by the College of Chemistry, University of California, Berkeley, CA. Single-crystal X-ray determinations were performed at CHEXRAY, University of California, Berkeley, CA.

$[TolC(NSiMe_3)_2]_2Ta(CH_2CH_3)(CH_3)I$ (3). $[TolC(NSiMe_3)_2]_2Ta(CH_2)CH_3$ (0.350 g, 0.458 mmol) was dissolved in toluene (45 mL) in a 100 mL round bottomed flask. Methyl iodide (85 μL, 1.4 mmol) was added using a microliter syringe. (From this point forward the reaction and workup were performed in the absence of light). The reaction mixture was stirred at room temperature for 7 h, during which time the solution turned green. The volatile materials were removed under reduced pressure and the product extracted with hexanes (50 mL). Concentration to 3 mL and cooling of the filtrate to −30 °C afforded green crystals (0.150 g, 36%). ^1H NMR (C_6D_6, 300 MHz): δ 0.268 (s, 36H, $Si(CH_3)_3$), 1.97 (s, 6H, $ArCH_3$), 2.12 (s, 3H, $TaCH_3$), 2.51 (q, $J = 7$ Hz, 2H, $TaCH_2CH_3$), 3.04 (t, $J = 7$ Hz, 3H, $TaCH_2CH_3$), 6.82 (d, $J = 8$ Hz, 4H, Ar), 7.39 (d, $J = 8$ Hz, 4H, Ar). Thermal instability prevented further characterization.

Reaction of $[TolC(NSiMe_3)_2]_2Ta(CH_2)CH_3$ with $CH_3C(O)H$. In the glove box, a tared vial was charged with **1** (10.0 mg, 0.0131 mmol) and 1,3,5-trimethoxybenzene (2.0 mg, 0.012 mmol). The solids were dissolved in C_6D_6 (0.5 mL) and transferred to an NMR tube equipped with a J. Young valve. Acetaldehyde (2.0 μL, 0.036 mmol) was added by syringe. The ^1H NMR spectrum that was obtained after 90 min contained peaks matching an authentic sample of $[TolC(NSiMe_3)_2]_2Ta(O)CH_3$, **12** (50% conversion *vs.* 1,3,5-trimethoxybenzene internal standard) and propylene. See later for full characterization of **12**.

$[TolC(NSiMe_3)_2]_2Ta[NC(CH_2)(C_6H_4CH_3)]CH_3$ (11a). A 100 mL round-bottomed flask was charged with $[TolC(NSiMe_3)_2]_2Ta(CH_2)CH_3$ (0.130 g, 0.170 mmol) and *p*-tolylnitrile (0.021 g, 0.18 mmol). Toluene (25 mL) was added and the orange solution was stirred overnight at room temperature. The volatile components were removed under reduced pressure and the product extracted into pentane (30 mL). The solution was filtered and concentrated to 2 mL. After cooling to −30 °C, off-white microcrystals were isolated by filtration (0.070 g, 46%). ^1H NMR (C_6D_6, 500 MHz): δ 0.179 (s, 36H, $Si(CH_3)_3$), 1.29 (s,

3H, TaCH_3), 1.96 (s, 6H, ArCH_3), 2.20 (s, 3H, ArCH_3), 5.27 (d, J = 1 Hz, 1H, TaNC(CH_aH$_b$)ArCH$_3$), 5.34 (d, J = 1 Hz, 1H, TaNC(CH_bH$_a$)ArCH$_3$), 6.84 (d, J = 8 Hz, 4H, Ar), 7.23 (d, J = 8 Hz, 2H, Ar), 7.25 (d, J = 8 Hz, 4H, Ar), 8.16 (d, J = 8 Hz, 2H, Ar). ^{13}C{^{1}H} (C$_6$D$_6$, 125 MHz): δ 3.0 (s, Si(CH_3)$_3$), 21.6 (s, ArCH_3), 21.7 (s, ArCH_3), 49.6 (s, TaCH_3), 105.3 (s, TaNC(CH_2)ArCH$_3$), 126.7 (s, Ar), 126.9 (s, Ar), 128.7 (s, Ar), 129.4 (s, Ar), 137.3 (s, Ar), 139.4 (s, Ar), 139.7 (s, Ar), 139.9 (s, Ar), 159.3 (s, TaNC(CH$_2$)ArCH$_3$), 180.2 (NCN). IR (cm^{-1}): 1612 (m), 1584 (m), 1543 (s), 1503 (s), 1344 (s), 1246 (s), 1184 (m), 1165 (m), 1150 (m), 1110 (m), 1026 (m), 1003 (s), 986 (s), 839 (s), 759 (s), 722 (s), 646 (m), 489 (m), 465 (m). Anal. Calc. for C$_{38}$H$_{62}$N$_5$Si$_4$Ta: C 51.73, H 7.08, N 7.94. Found C 52.02, H 7.18, N 7.83%.

NMR-scale reaction of 1 with CH$_3$CN. Complex **1** (7.5 mg, 0.0098 mmol) and 1,3,5-trimethoxybenzene (1.6 mg, 0.0095 mmol) were weighed into a tared vial. The solids were dissolved in approx. 0.5 mL C$_6$D$_6$ and the solution was transferred to an NMR tube equipped with a J. Young valve. Acetonitrile (1.0 μL, 0.019 mmol) was added to the NMR tube using a microliter syringe. After 24 h at room temperature, the ^{1}H NMR spectrum showed peaks corresponding to [TolC(NSiMe$_3$)$_2$]$_2$Ta[NC(CH$_2$)(CH$_3$)]CH$_3$ (**11b**) (conversion >99% *vs.* 1,3,5-trimethoxybenzene internal standard). ^{1}H NMR (C$_6$D$_6$, 300 MHz): δ 0.188 (s, 36H, Si(CH_3)$_3$), 1.16 (s, 3H, TaCH_3), 1.98 (s, 6H, ArCH_3), 2.13 (s, 3H, TaNC(CH$_2$)CH_3), 4.42 (br s, 1H, TaNC(CH_aH$_b$)CH$_3$), 4.75 (br s, 1H, TaNC(CH_bH$_a$)CH$_3$), 6.83 (d, J = 8 Hz, 4H, Ar), 7.14 (d, J = 8 Hz, 4H, Ar).

[TolC(NSiMe$_3$)$_2$]$_2$Ta[η^2-N(2,6-dimethylphenyl)C(CH$_2$)]CH$_3$ (13). A 50 mL round bottomed flask was charged with **1** (0.200 g, 0.261 mmol) and 2,6-dimethylphenyl isocyanide (0.035 g, 0.27 mmol). The solids were cooled to −20 °C and toluene (20 mL) was added to dissolve them. The yellow solution was stirred first at −20 °C and then at room temperature for 3 $\frac{1}{2}$ h. The volatile materials were removed under reduced pressure and the residue was extracted into diethyl ether (20 mL). The solution was filtered, concentrated to 5 mL, and cooled to −30 °C. Orange crystals were isolated by filtration (0.120 g, 51%). ^{1}H NMR (C$_6$D$_6$, 500 MHz): δ 0.143 (s, 36 H, Si(CH_3)$_3$), 1.22 (s, 3H, TaCH_3), 1.97 (s, 6H, ArCH_3), 2.57 (s, 6H, NAr(CH_3)$_2$), 4.78 (s, 1H, CH_aH$_b$), 5.99 (s, 1H, CH$_a$$H_b$), 6.81 (d, 4H, J = 8 Hz, *Ar*), 7.07 (t, 1H, J = 8 Hz, *Ar*), 7.20 (d, 2H, J = 8 Hz, *Ar*), 7.25 (d, 4H, J = 8 Hz, *Ar*). ^{13}C{^{1}H} (C$_6$D$_6$, 125 MHz): δ 3.4 (s, Si(CH_3)$_3$), 21.0 (s, ArCH_3), 21.6 (s, NAr(CH_3)$_2$), 63.3 (s, TaCH_3), 77.2 (s, CH_2), 125.5 (s, *Ar*), 127.3 (s, Ar), 129.3 (s, *Ar*), 133.3 (s, *Ar*), 139.0 (s, *Ar*), 139.8 (s, *Ar*), 152.1 (s, Ar), 182.2 (s, NCN), 206.0 (s, TaCNAr). DEPT-135 77.2 (inverted). IR (cm^{-1}): 2854 (s), 1611 (w), 1581 (w), 1518 (w), 1406 (m), 1358 (s), 1265 (m), 1246 (s), 1163 (w), 1004 (m), 985 (s), 836 (s), 764 (m), 710 (m) 643 (w). EI-MS (*m*/*z*): 895.8 (M$^+$). Anal. Calc. For C$_{39}$H$_{64}$N$_5$Si$_4$Ta: C 52.21, H 7.30, N 7.81. Found C 51.98, H 7.62, N 7.70%.

[TolC(NSiMe$_3$)$_2$]$_2$Ta(SCH$_2$)CH$_3$ (14). Compound **1** (0.207 g, 0.271 mmol) was loaded into a 100 mL round-bottomed flask. Toluene (13 mL) was added to dissolve the solid. Propylene sulfide (0.100 mL, 1.28 mmol) was added by syringe to the orange solution at room temperature. After stirring for 20 h, the volatile materials were removed under reduced pressure. The yellow solid was extracted into pentane (50 mL). The solution was filtered, concentrated to 10 mL and cooled to −30 °C. Yellow needles were isolated by filtration (0.120 g, 55%). ^{1}H NMR (C$_6$D$_6$, 500 MHz): δ 0.137 (s, 36 H, Si(CH_3)$_3$), 1.11 (s, 3H, TaCH_3), 1.96 (s, 6H, ArCH_3), 2.87 (s, 2H, SCH_2), 6.80 (d, 4H, J = 8 Hz, *Ar*), 7.14 (d, 4H, J = 8 Hz, *Ar*). ^{13}C{^{1}H} (C$_6$D$_6$, 125 MHz): δ 3.1 (s, Si(CH_3)$_3$), 21.6 (s, ArCH_3), 57.3 (s, TaCH_3), 71.1 (s, SCH$_2$), 126.9 (s, *Ar*), 129.3 (s, *Ar*), 138.9 (s, *Ar*), 139.5 (s, *Ar*), 180.2 (s, NCN). DEPT-135 71.1 (inverted). IR (cm^{-1}): 1612 (m), 1524 (m), 1346 (m), 1246 (s), 1178 (w), 1158 (w), 1026 (w), 1007 (m), 985 (s), 839 (s), 761 (s), 716 (s), 644 (m), 462 (m). Anal. Calc. For C$_{30}$H$_{55}$N$_4$Si$_4$STa: C 45.20, H 6.95, N 7.03. Found C 44.88, H 6.82, N 6.94%.

[TolC(NSiMe$_3$)$_2$]$_2$Ta(S)CH$_3$ (15). A 100 mL round-bottomed flask was charged with **1** (0.100 g, 0.131 mmol) and Ph$_3$CSH (0.037 g, 0.13 mmol). Toluene (20 mL) was added to the solids at −30 °C. The yellow solution was slowly warmed to room temperature overnight. The volatile materials were removed under reduced pressure and the yellow solid was extracted into diethyl ether (15 mL). The solution was filtered, concentrated to 1 mL and cooled to −30 °C. Yellow microcrystals of **15** were isolated by filtration (0.60 g, 60%). ^{1}H NMR (C$_6$D$_6$, 500 MHz): δ 0.256 (s, 36H, Si(CH_3)$_3$), 1.67 (s, 3H, TaCH_3), 1.97 (s, 6H, ArCH_3), 6.80 (d, J = 8 Hz, 4H, Ar), 7.16 (d, J = 8 Hz, 4H, Ar). ^{13}C{^{1}H} NMR (C$_6$D$_6$, 125 MHz): δ 3.0 (s, Si(CH_3)$_3$), 21.6 (s, ArCH_3), 56.4 (s, TaCH_3), 126.6 (s, Ar), 129.4 (s, Ar), 138.9 (s, Ar), 139.7 (s, Ar), 181.3 (NCN). EI-MS (*m*/*z*): 782 (M$^+$). Anal. Calc. for C$_{29}$H$_{53}$N$_4$Si$_4$STa: C 44.48, H 6.82, N 7.15. Found C 44.32, H 6.58, N 6.85%.

Preparation of Ph$_3$CSD. The following procedure is a modification of that reported for n-hexanethiol-d_1.[53] A 50 mL Schlenk round bottom flask was charged with Ph$_3$CSH (0.500 g, 1.81 mmol). Under a purge of N$_2$, dry diethyl ether (20 mL) was added to the flask. The thiol dissolved with gentle heating. NaH (0.045 g, 1.9 mmol) was added and the reaction mixture was stirred until the bubbling ceased (35 min). D$_2$O (1.0 mL) was added by pipette, forming a biphasic solution which was stirred vigorously for 30 min. The ether layer was removed using a separatory funnel and dried over MgSO$_4$. The ether solution was concentrated to yield white crystals (0.420 g, 84%). Isotopic enrichment as determined by ^{1}H NMR = 73% d$_1$.

NMR-scale reaction of 1 with Ph$_3$CSD. In the glove box, a tared vial was charged with **1** (0.0101 g, 0.0132 mmol) and 1,3,5-trimethoxybenzene (0.0024 g, 0.014 mmol). C$_6$D$_6$ (approx. 0.5 mL) was added to dissolve the solids and the solution was transferred to a NMR tube equipped with a J. Young valve. An ^{1}H NMR spectrum was acquired. In the glove box, Ph$_3$CSD (0.0037 g, 0.013 mmol) was added to the C$_6$D$_6$ solution. After 3.5 h, during which time the reaction solution turned yellow, the ^{1}H NMR spectrum showed >99% conversion to the products, **7** and triphenylethane. Isotopic incorporation was observed in the methyl groups of both the metal-containing and organic products (see text for further details). Relevant ^{1}H NMR (300 MHz) resonances are as follows: δ 1.62 (br t, 0.442 H, TaCH_2D), 1.65 (s, 1.15 H, TaCH_3), 2.01 (br t, 0.0438 H, Ph$_3$CCH_2D), 2.03 (s, 1.09 H, Ph$_3$CCH_3). Resonances for Ph$_3$CCH$_3$ matching the literature were observed in the ^{13}C{^{1}H} NMR, but peaks for the Ph$_3$CCH$_2$D were not definitely resolvable from noise.

Characterization of methylpyridine products from the reaction of 1 with substituted pyridine *N*-oxides.

(a) Typical procedure: Reaction with pyridine N-oxide. In the glove-box, $[TolC(NSiMe_3)_2]_2Ta(CH_2)CH_3$ (0.075 g, 0.098 mmol) and pyridine *N*-oxide (0.0093 g, 0.098 mmol) were weighed into a tared vial. C_6D_6 (0.5 mL) was added to dissolve the reagents. After 14 h, ^1H and $^{13}C\{^1H\}$ NMR spectra were obtained of this reaction mixture. These spectra contained peaks matching authentic samples of **12** and 2-methylpyridine.[26] Conversion by ^1H NMR: 99%.

(b) Reaction with 2-methylpyridine N-oxide. ^1H and $^{13}C\{^1H\}$ NMR spectra matched those for an authentic sample of 2,6-dimethylpyridine. Conversion by ^1H NMR: 99%.[26]

(c) Reaction with 2-ethylpyridine N-oxide. The ^1H NMR spectrum contained peaks consistent with 6-ethyl-2-methylpyridine. Conversion by ^1H NMR: 90%. Relevant ^1H NMR (300 MHz): δ 1.26 (t, $J = 7$ Hz, 2H, CH_2CH_3), 2.42 (s, 3H, CH_3), 2.79 (q, $J = 7$ Hz, 3H, CH_2CH_3), 6.19 (m, 1H, Ar), 6.27 (m, 1H, Ar), 6.60 (m, 1H, Ar).

(d) Reaction with 2,2′-dipyridyl N-oxide. The ^1H NMR spectrum contained peaks consistent with 6-methyl-2,2′-dipyridyl. Conversion by ^1H NMR: 95%. Relevant ^1H NMR (300 MHz): δ 2.45 (s, 3H, CH_3), 6.67 (m, 2H, Ar), 7.24 (m, 2H, Ar), 8.53 (m, 1H, Ar), 8.64 (d, $J = 8$ Hz, 1H, Ar), 8.75 (d, $J = 8$ Hz, 1H, Ar).

General experimental details for X-ray structure determinations

Crystals were mounted onto glass fibers using Paratone N hydrocarbon oil and were transferred to a Siemens SMART diffractometer/CCD area detector,[54] centered in the beam, and cooled by a nitrogen-flow low-temperature apparatus. Preliminary orientation matrix and cell constants were determined by collection of 60 10 s frames, followed by spot integration and least squares refinement. A hemisphere of data was collected using ω scans of 0.3° counted for a total of 10 s per frame. The raw data were integrated by the program SAINT.[55] Data analysis was performed using XPREP.[56] For **13**, and **14**, an absorption correction was applied using XPREP; for **1** and **15**, the correction was applied using SADABS.[57] The unit cell parameters and statistical analysis of the intensity distribution were used for space group determination.[58] The data were corrected for Lorentz and polarization effects, but no correction for crystal decay was applied. Unique equivalent reflections were merged. The structures were solved by direct methods[59] and expanded using Fourier techniques.[60] Except as noted, all non-hydrogen atoms were refined anisotropically and hydrogen atoms were included as fixed contributions but not refined. The quantity minimized by the least-squares program was $\Sigma w(|F_o| - |F_c|)^2$ where w is the weight of a given observation. The weighting scheme was based on counting statistics and included a factor ($p = 0.030$) to downweight the intense reflections. The analytical forms of the scattering factor tables for the neutral atoms were used,[61] and all scattering factors were corrected for both the real and imaginary components of anomalous dispersion.[62] All calculations were performed using the teXsan[63] crystallographic software package of Molecular Structure Corp. Detailed information regarding disordered atoms in individual structure solutions is given below.

For **1**, the complex resides on a crystallographic C_2 axis that passes through Ta1. Therefore, the tantalum-bound methylene and methyl groups of **1** are disordered; C1 was refined anisotropically at full occupancy to account for both of these ligands.

As in **1**, **14** also resides on a crystallographic C_2 axis that passes through Ta1; C15 represents the disordered Ta–(CH_2S) and Ta–CH_3 carbon atoms; it was refined isotropically at full occupancy. The sulfur atom, S1, was disordered over two sites; it was refined isotropically at half-occupancy. Carbon atoms C2–C4 and C16–C18 of **14** are part of a disordered trimethylsilyl group; each atom was refined isotropically at half-occupancy.

Like in **1** and **14**, complex **15**, resides on a crystallographic C_2 axis that passes through Ta1. The Ta–CH_3 carbon atom, C15, is also positionally disordered; it was refined isotropically at half-occupancy. The sulfur atom, S1, was disordered in a similar manner; it was refined anisotropically at half-occupancy.

CCDC reference numbers 283319–283322.

For crystallographic data in CIF or other electronic format see DOI: 10.1039/b512741f

Acknowledgements

This work was supported by grants from the National Science Foundation (CHE-0345488 to R. G. B.) and (CHE-0072819 to J. A.). We thank Dr Fred Hollander for expert assistance with the X-ray solution and refinement.

References

1 P. M. Maitlis, H. C. Long, R. Quyoum, M. L. Turner and Z.-Q. Wang, *Chem. Commun.*, 1996, 1.
2 M. J. Overett, R. O. Hill and J. R. Moss, *Coord. Chem. Rev.*, 2000, **206–207**, 581.
3 J. P. Collman, L. S. Hegedus, J. R. Norton and R. G. Finke, in *Principles and Applications of Organotransition Metal Chemistry*, Mill Valley, CA, 1987.
4 J. Toyir, M. Leconte, G. P. Niccolai and J. M. Basset, *J. Catal.*, 1995, **152**, 306.
5 W. A. Nugent and J. M. Mayer, *Metal–Ligand Multiple Bonds*, John Wiley & Sons, New York, 1988.
6 M. P. Doyle and M. N. Protopopova, *Tetrahedron*, 1998, **54**, 7919.
7 R. R. Schrock, *Acc. Chem. Res.*, 1979, **12**, 98.
8 R. R. Schrock and P. R. Sharp, *J. Am. Chem. Soc.*, 1978, **100**, 2389.
9 R. R. Schrock, *J. Am. Chem. Soc.*, 1975, **97**, 6577.
10 C. D. Wood, S. J. McLain and R. R. Schrock, *J. Am. Chem. Soc.*, 1979, **101**, 3210.
11 R. R. Schrock, *Science*, 1983, **219**, 13.
12 F. N. Tebbe, G. W. Parshall and G. S. Reddy, *J. Am. Chem. Soc.*, 1978, **100**, 3611.
13 K. A. Brown-Wensley, S. L. Buchwald, L. Cannizzo, L. Clawson, S. Ho, D. Meinhardt, J. R. Stille and R. H. Grubbs, *Pure Appl. Chem.*, 1983, **55**, 1733.
14 M. D. Fryzuk, X. Gao, K. Joshi, P. A. MacNeil and R. L. Massey, *J. Am. Chem. Soc.*, 1993, **115**, 10581.
15 M. D. Fryzuk, S. A. Johnson and S. J. Rettig, *Organometallics*, 1999, **18**, 4059.
16 A. H. Lui, R. C. Murray, J. C. Dewn, B. D. Santarsiero and R. R. Schrock, *J. Am. Chem. Soc.*, 1987, **109**, 4282.
17 L. Andrews, H. G. Cho and X. Wang, *Inorg. Chem.*, 2005, **44**, 4834.
18 J. J. Eisch and A. A. Adeosun, *Eur. J. Org. Chem.*, 2005, 993.
19 A. E. Enriquez, P. S. White and J. L. Templeton, *J. Am. Chem. Soc.*, 2001, **123**, 4992.
20 R. H. Crabtree, *The Organometallic Chemistry of the Transition Metals*, John Wiley and Sons, New York, 1994.
21 D. P. Klein and R. G. Bergman, *J. Am. Chem. Soc.*, 1989, **111**, 3079.
22 J. C. Hayes, P. Jernakoff, G. A. Miller and N. J. Cooper, *Pure Appl. Chem.*, 1984, **56**, 25.
23 A. F. Hill, W. R. Roper, J. M. Waters and A. H. Wright, *J. Am. Chem. Soc.*, 1983, **105**, 5939.
24 D. Y. Dawson and J. Arnold, *Organometallics*, 1997, **16**, 1111.

25 R. Duchateau, C. Van Wee, A. Meetsma, P. van Duijen and J. Teuben, *Organometallics*, 1996, **15**, 3539.
26 S. M. Mullins, R. G. Bergman and J. Arnold, *Organometallics*, 1999, **18**, 4465.
27 K. C. Nicolaou, A. E. Koumbis, S. A. Snyder and K. B. Simonsen, *Angew. Chem., Int. Ed.*, 2000, **39**, 2529.
28 K. C. Nicolaou, S. A. Snyder, X. H. Huang, K. B. Simonsen, A. E. Koumbis and A. Bigot, *J. Am. Chem. Soc.*, 2004, **126**, 10162.
29 The coordination aperture is defined as the angle between the two planes through the metal center that touch the inner van der Waals surface of the ligand system.
30 T. Takeda, *Bull. Chem. Soc. Jpn.*, 2005, **78**, 195.
31 R. R. Schrock and J. D. Fellmann, *J. Am. Chem. Soc.*, 1978, **100**, 3359.
32 R. R. Schrock, L. W. Messerle, C. D. Wood and L. J. Guggenberger, *J. Am. Chem. Soc.*, 1978, **100**, 3793.
33 R. R. Schrock, *J. Am. Chem. Soc.*, 1976, **98**, 5399.
34 G. Wittig, *J. Organomet. Chem.*, 1975, **100**, 279.
35 G. Wittig and G. Geissler, *Justus Liebigs Ann. Chem.*, 1954, **580**, 44.
36 S. J. McLain, C. D. Wood and R. R. Schrock, *J. Am. Chem. Soc.*, 1976, **98**, 3519.
37 R. Aumann, *Angew. Chem., Int. Ed. Engl.*, 1988, **27**, 1456.
38 D. R. Lide, in *Handbook of Chemistry and Physics*, CRC Press, Boca Raton, FL, 1996.
39 Rotation around the internal C_2 axis has been observed in amidinate complexes. See: L. A. Koterwas, J. C. Fettinger and L. R. Sita, *Organometallics*, 1999, **18**, 4183.
40 The assignments of the individual tolyl methyl (c, d) and trimethylsilyl groups (e, f, g) are not conclusively known, but are instead based on the X-ray structure.
41 J. E. Nelson, G. Parkin and J. E. Bercaw, *Organometallics*, 1992, **11**, 2181.
42 S. L. Buchwald, R. B. Nielson and J. C. Dewan, *J. Am. Chem. Soc.*, 1987, **109**, 1590.
43 J. W. Park, L. M. Henling, W. P. Schaefer and R. H. Grubbs, *Organometallics*, 1990, **9**, 1650.
44 G. Parkin, E. Bunel, B. J. Burger, M. S. Trimmer, A. van Asselt and J. E. Bercaw, *J. Mol. Catal.*, 1987, **41**, 21.
45 M. G. B. Drew, D. A. Rice and D. M. Williams, *J. Chem. Soc., Dalton Trans.*, 1984, 845.
46 G. Parkin, *Prog. Inorg. Chem.*, 1998, **47**, 1.
47 The sums of $TaCH_3$ and $TaCH_2$ integrations relative to trimethoxybenzene internal standard are: 3.35 H (start) and 3.12 H (finish).
48 H. Kawaguchi and K. Tatsumi, *Organometallics*, 1997, **16**, 307.
49 K. Tatsumi, A. Tahara and A. Nakamura, *J. Organomet. Chem.*, 1994, **471**, 111.
50 P. J. Alaimo, D. W. Peters, J. Arnold and R. G. Bergman, *J. Chem. Educ.*, 2001, **78**, 64.
51 L. Kaczmarek, R. Balicki and P. Nantka-Namirski, *Chem. Ber.*, 1992, **125**, 1965.
52 D. Wenkert and R. B. Woodward, *J. Org. Chem.*, 1983, **48**, 283.
53 D. Plant, D. S. Tarbell and C. Whiteman, *J. Am. Chem. Soc.*, 1955, **77**, 1572.
54 *SMART: Area-Detector Software Package*, Siemens Industrial Automation, Inc., Madison, WI, 1995.
55 *SAINT: SAX Area-Dectector Integration Program, V4.024*, Siemens Industrial Automation, Inc., Madison, WI, 1995.
56 *XPREP: (v 5.03) Part of the SHELXTL Crystal Structure Determination Siemens Industrial Automation, Inc.*, Madison, WI, 1995.
57 G. M. Sheldrick, *SADABS: Siemens Area Detector ABSorption correction program*, 1996. Advance copy, private communication.
58 D. T. Cromer and J. T. Waber, *International Tables for X-ray Crystallography*, The Kynoch Press, Birmingham, England, 1974, vol. IV, table 2.2 A.
59 SIR92: A. Altomare, M. C. Burla, Camalli, M. Cascarano, C. Giacovazzo, A. Guagliardi and G. Polidori, *J. Appl. Crystallogr.*, 1993, **26**, 343.
60 DIRDIF92: P. T. Beurskens, G. Admiraal, G. Beurskens, W. P. Bosman, S. Garcia-Granda, R. O. Gould, J. M. M. Smits and C. Smykalla, *The DIRDIF program system, Technical Report of the Crystallography Laboratory*, University of Nijmegen, The Netherlands, 1992.
61 D. C. Creagh and J. H. Hubbell, *International Tables for Crystallography*, Vol C, ed. A. J. C. Wilson, Kluwer Academic Publishers, Boston, MA, 1992, Table 4.2.4.3, pp. 200–206.
62 J. A. Ibers and W. C. Hamilton, *Acta Crystallogr.*, 1964, **17**, 781.
63 *teXsan: Crystal Structure Analysis Package*, Molecular Structure Corporation, The Woodlands, TX, 1985 and 1992.

